Food & Function

ROYAL SOCIETY OF CHEMISTRY

PAPER

View Article Online
View Journal | View Issue

Cite this: *Food Funct.*, 2024, **15**, 2996

3,4′,5-Trimethoxy-*trans*-stilbene ameliorates hepatic insulin resistance and oxidative stress in diabetic obese mice through insulin and Nrf2 signaling pathways†

Yi Tan,[a] Chunxiu Zhou,[a] Lingchao Miao,[a] Xutao Zhang,[a] Haroon Khan,[b] Baojun Xu*[c] and Wai San Cheang *[a]

Resveratrol has profound benefits against diabetes. However, whether its methylated derivative 3,4′,5-trimethoxy-*trans*-stilbene (3,4′,5-TMS) also plays a protective role in glucose metabolism is not characterized. We aimed to study the anti-diabetic effects of 3,4′,5-TMS *in vitro* and *in vivo*. Insulin-resistant HepG2 cells (IR-HepG2) were induced by high glucose plus dexamethasone whilst six-week-old male C57BL/6J mice received a 60 kcal% fat diet for 14 weeks to establish an obese diabetic model. 3,4′,5-TMS did not reduce the cell viability of IR-HepG2 cells at concentrations of 0.5 and 1 μM, which enhanced the capability of glycogen synthesis and glucose consumption in IR-HepG2 cells. Four-week oral administration of 3,4′,5-TMS at 10 mg kg^{-1} day^{-1} ameliorated insulin sensitivity and glucose tolerance of diet-induced obese (DIO) mice. 3,4′,5-TMS activated the phosphatidylinositol 3-kinase (PI3K)/protein kinase B (Akt) pathway by inhibiting phosphorylation of insulin receptor substrate (IRS)-1 at Ser307 and increasing the protein levels of IRS-1 and IRS-2 to restore the insulin signaling pathway in diabetes. 3,4′,5-TMS also upregulated the phosphorylation of glycogen synthase kinase 3 beta (GSK3β) at Ser9. 3,4′,5-TMS suppressed oxidative stress by increasing the protein levels of nuclear factor erythroid 2-related factor 2 (Nrf2), heme oxygenase-1 (HO-1) and NAD(P)H : quinone oxidoreductase 1 (NQO1) and antioxidant enzyme activity. In summary, 3,4′,5-TMS alleviated hepatic insulin resistance *in vitro* and *in vivo*, by the activation of the insulin signaling pathway, accomplished by the suppression of oxidative stress.

Received 7th October 2023,
Accepted 9th February 2024

DOI: 10.1039/d3fo04158a

rsc.li/food-function

Introduction

According to the World Health Organization statistics, over 400 million people are suffering from diabetes mellitus worldwide and the morbidity has a youth-oriented tendency. Type 2 diabetic mellitus (T2DM) is a chronic metabolic disease and is often linked to unhealthy lifestyles, such as high consumption of fat and a sedentary lifestyle,[1] accounting for about 90% of diabetes cases.[2] High blood glucose levels and insulin resistance are fundamental features of T2DM, which is a leading cause of death in humans and puts pressure on the healthcare system and social economy.[3] Insulin resistance is characterized as a state in which cells in the liver, muscle and fat become less sensitive to insulin and insulin cannot produce normal biological effects. In insulin resistance, insulin signaling in the liver is blocked, resulting in liver function impairment, inhibition of hepatic glycogen synthesis, and increased gluconeogenesis.[4] At the same time, impaired insulin signaling normally disrupts lipid metabolism, resulting in reduced lipid storage capacity in adipocytes, increased lipid breakdown, and elevated levels of free fatty acids (FFAs) in plasma and tissue.[5] Taken together, T2DM is related to obesity, fatty liver, cardiovascular disease, *etc.*, because of a high level of blood glucose and ectopic lipid accumulation.[6–8]

Phosphatidylinositol 3-kinase (PI3K)/protein kinase B (Akt) signaling plays a crucial role in insulin signal transduction, mediated by insulin receptor substrate (IRS)-induced serine and/or threonine phosphorylation.[9] This pathway promotes glycogen synthesis and reduces hepatic gluconeogenesis by regulating downstream proteins such as glycogen synthase

[a]*Institute of Chinese Medical Sciences, State Key Laboratory of Quality Research in Chinese Medicine, University of Macau, Macau SAR, China. E-mail: annacheang@um.edu.mo*
[b]*Department of Pharmacy, Abdul Wali Khan University Mardan, Mardan 23200, Pakistan*
[c]*Food Science and Technology Program, BNU-HKBU United International College, Zhuhai, Guangdong, China. E-mail: baojunxu@uic.edu.cn*

† Electronic supplementary information (ESI) available. See DOI: https://doi.org/10.1039/d3fo04158a

kinase-3 beta (GSK3β) and Forkhead box-O1 (FOXO1).[10] Insulin resistance in the liver correlates with the abundance status of IRS1 and IRS2, which complement each other during metabolism.[11,12] Ser307 phosphorylation of IRS1 impairs PI3K/Akt signaling to block insulin signaling by reducing coupling between IRS1 and the insulin receptor as well as the P85 domain of PI3K.[13,14] On the other side, reactive oxygen species (ROS) production is stimulated by high levels of glucose and FFAs in diabetes.[15] ROS generation mainly occurs within mitochondria and the liver is a mitochondria-rich site, thus inducing hepatic oxidative stress.[16,17] Oxidative stress damages proteins, lipids and DNA, induces cell apoptosis and endoplasmic reticulum (ER) stress, and thereby exacerbates insulin resistance.[16] The nuclear factor erythroid 2-related factor 2 (Nrf2), an important mediator for the antioxidant defense mechanism, protects organs and cells from damage by oxidative stress in diabetes.[18,19] Nrf2 is a key downstream target of the PI3K/Akt pathway, which promotes Nrf2 dissociation from Kelch-like ECH-associated protein 1 (Keap1) to translocate into the nucleus.[19] Next, Nrf2 initiates the transcription of a series of downstream genes, including heme oxygenase-1 (HO-1) and NAD(P)H : quinone oxidoreductase 1 (NQO1), thereby triggering crucial cellular processes including the antioxidant response, detoxification metabolism, and cellular repair.[19] A lack of Nrf2 or decreasing Nrf2 is connected with insulin secretion and resistance.[20,21] The redox-sensitive signaling system is considered as an important target for antidiabetes therapy.[22]

Resveratrol, a natural compound found in various plants, including red wine, grape skins, blueberries, and other fruits and nuts, is a polyphenolic compound with potential health benefits, such as anticancer, cardioprotective, neuroprotective, and antioxidant properties.[23,24] However, there are shortcomings in the pharmacokinetic profile of resveratrol, including low bioavailability and a short half-life, necessitating frequent intake or administration for sustained effects. Additionally, the low solubility of resveratrol may affect its dissolution and stability in formulations.[25] Structural modifications can improve the properties of compounds. Methoxy substitution of the hydroxyl group in resveratrol has been shown in previous studies to enhance bioavailability and stability, modulate pharmacological activity, and improve physicochemical properties, providing a foundation for the development of safer and more effective treatment methods and medications.[26] As a methoxy derivative of resveratrol, 3,4′,5-trimethoxy-*trans*-stilbene (3,4′,5-TMS) shows enhanced plasma levels, lower systemic clearance and prolonged half-life, addressing the limitations of resveratrol in pharmacokinetics.[27] It is known to possess potent anti-inflammatory, antioxidant, anticancer, and vascular protective activities.[28–31] However, there are very few studies on this compound in diabetes. Herein, our present study aimed to explore the anti-diabetic effect and the underlying mechanism of 3,4′,5-TMS in insulin-resistant HepG2 cells (IR-HepG2) induced by high glucose plus dexamethasone (DXMS) and in high-fat diet-induced obese (DIO) mice.

Materials and methods

Chemicals and reagents

Dimethyl sulfoxide (DMSO) was obtained from Hangzhou Fude Biological Technology Co. Ltd (Zhejiang, Hangzhou, China), while ethanol, sodium chloride (NaCl), potassium chloride (KCl), dibasic sodium phosphate (Na_2HPO_4) and potassium dihydrogen phosphate (KH_2PO_4) were purchased from Sinopharm Chemical Reagent Co., Ltd (Shanghai, China). Dexamethasone (DXMS), D-glucose (≥99.5%), tris(hydroxymethyl)aminomethane (Tris), Tween® 20 detergent and sodium carboxymethyl cellulose (CMC–Na) were obtained from Sigma–Aldrich (St Louis, MO, USA). 3,4′,5-TMS (purity > 98%) was acquired from Tokyo Chemical Industry Co., Ltd (Tokyo, Japan). Reagents for preparing SDS-PAGE gels were acquired from Bio-Rad (Hercules, CA, USA): *N*,*N*,*N*′,*N*′ tetramethylethylene-diamine (TEMED), ammonium persulfate (APS), 30% acrylamide/bis solution, 1.5 M Tris-HCl (pH 8.8), 10% SDS Solution, 0.5 M Tris-HCl (pH 6.8), and isopropyl alcohol.

HepG2 cell culture and drug treatments

HepG2 cells were acquired from the Chinese Academy of Sciences (Shanghai, China). The cells were cultured with low-glucose Dulbecco's modified Eagle's medium (DMEM) supplemented with 10% fetal bovine serum (FBS), penicillin–streptomycin, and non-essential amino acids (NEAAs) which were obtained from Gibco (Carlsbad, CA, USA). The cells were maintained at 37 °C in a 5% CO_2 humidified incubator. An insulin resistant cell model was triggered by a combination of DXMS and high glucose as previously reported.[32,33] DXMS exacerbates the onset of insulin resistance and oxidative stress in a hyperglycemic environment by interfering with insulin signaling and impairing mitochondrial function.[34] HepG2 cells were pretreated with DXMS (30 μM, dissolved in ethanol) and D-glucose (50 mM final concentration) for 48 h. Thereafter, the experimental groups were treated with different concentrations of 3,4′,5-TMS (0.5 and 1 μM) for 16 h. The group not treated with DXMS, D-glucose and 3,4′,5-TMS served as the control.

Cell viability assay

The cytotoxic effect of 3,4′,5-TMS on HepG2 cells was measured by the 3-(4,5-dimethylthiazol-2-yl)-2,5-diphenyltetrazolium bromide (MTT) assay; the MTT reagent was obtained from Sigma-Aldrich (St Louis, MO, USA). According to the manufacturer's instructions, HepG2 cells (7×10^3 cells per well) were seeded on 96-well culture plates and cultured overnight. Then the cells were incubated with different concentrations of 3,4′,5-TMS (0.5, 1, 2.5, 5, 10, 25, and 50 μM) for 48 h. At the same time, the effect of solvent DMSO was tested. A group with no treatment served as the control. After incubation, the cells were refreshed with 10% MTT-containing medium at 37 °C for 3 h. At last, the supernatants were discarded and 150 μL of DMSO was added to each well to dissolve the formazan crystals by shaking the culture plate for 30 min.

The absorbance was read at 570 nm using a SpectraMax M5 microplate reader (Molecular Devices, Silicon Valley, CA, United States). The relative cell viability was calculated as the percentage of the control group.

Glucose consumption assay

The effect of 3,4′,5-TMS on glucose consumption potency was determined using a glucose assay kit, which was obtained from Nanjing Jiancheng Bioengineering Institute (Nanjing, Jiangsu, China). 6-Well culture plates were used to seed and culture HepG2 cells overnight with a density of 7×10^5 cells per well. The cells were administered DXMS plus D-glucose for 48 h as well as different concentrations of 3,4′,5-TMS (0.1, 0.5 and 1 μM) for 16 h. According to the manufacturer's instructions, the supernatants were collected and their glucose concentrations were measured using the kit. The absorbance at 505 nm was detected with a microplate spectrophotometer. The result was calculated as below: glucose consumption = glucose concentration of blank – glucose concentration of each treatment group.

Glycogen synthesis assay

The effect of 3,4′,5-TMS on the glycogen synthesis ability was determined using a glycogen assay kit (Nanjing Jiancheng, Nanjing, Jiangsu, China). HepG2 cells were cultured and treated with 3,4′,5-TMS (0.5 and 1 μM) in 6-well culture plates as previously described. According to the manufacturer's instructions, the cells were collected and their intracellular glycogen contents were detected using the kit. The absorbance at 620 nm was detected with a microplate spectrophotometer.

Determination of the reactive oxygen species (ROS) level

The intracellular ROS of HepG2 cells was determined by 5-(and-6)-chloromethyl-2′,7′-dichlorodihydrofluorescein diacetate acetyl ester (CM-H_2DCFDA) that was acquired from Invitrogen (Carlsbad, CA, USA). HepG2 cells (5×10^4 cells per well) were seeded on 24-well culture plates and cultured overnight. After treatment with DXMS, D-glucose and different concentrations of 3,4′,5-TMS, the cells were washed with PBS. Incubating with normal physiological saline solution (NPSS) that contained 10 μM CM-H_2DCFDA at 37 °C for 30 min in the dark, the fluorescence images were captured using a Leica-DMi8 inverted fluorescence microscope (Leica Microsystems, Wetzlar, Germany) at 488/525 nm (excitation/emission). The fluorescence intensity of CM–H_2DCFDA was quantified using ImageJ software (National Institutes of Health, Bethesda, MD, USA).

Diet-induced obese model and 3,4′,5-TMS treatments

Six-week-old male C57BL/6J mice (n = 18) were housed under controlled conditions with a temperature of 22–24 °C and a 12 h light/dark cycle, and were assigned to three different dietary groups (n = 6 per group). All animal experiments were performed in compliance with the 'Animal Research: Reporting In Vivo Experiments' (ARRIVE) 2.0 guidelines and approved by the Animal Research Ethics Committee of University of Macau (approval number UMARE-024-2021). A diet-induced obese (DIO) model was established by receiving a fat-diet containing 60 kcal% fat (D12492, Research diets, Sysebio, China) for 14 weeks. Oral administration of suspending agents CMC–Na (vehicle) and 3,4′,5-TMS at 10 mg per kg body weight were supplied daily to DIO mice by gavage for the last four weeks. A standard-chow diet was given to the control mice with the administration of vehicle for 4 weeks.

Blood glucose measurements

The oral glucose tolerance test (OGTT) was performed in all groups of mice after 6 h of fasting. The mice were gavaged with glucose solution (1.2 g per kg body weight, Sigma-Aldrich, St Louis, MO, USA). Blood samples were collected from the caudal vein of mice and blood glucose concentrations were analyzed at 0, 15, 30, 45, 60, 90 and 120 min using a commercial glucometer (Jiangsu Yuyue Medical Equipment and Supply Co., Ltd, Shanghai, China). For the insulin tolerance test (ITT), the mice were fasted for 2 hours and then intra-peritoneally injected with 0.5 U per kg body weight insulin that was acquired from Sigma-Aldrich (St Louis, MO, USA). The blood glucose concentrations were measured at the same time point as the OGTT.

Biochemical analysis in plasma and the liver

Mice were sacrificed by CO_2 asphyxiation after chronic treatment. Blood samples were collected from the inferior vena cava of mice into prechilled heparin-coated microcentrifuge tubes, followed by centrifugation at 3000 rpm at 4 °C for 10 min to obtain the plasma. The levels of alanine aminotransferase (ALT) and aspartate aminotransferase (AST) in plasma were determined using Nanjing Jiancheng kits (Nanjing, Jiangsu, China, C009-2-1 and C010-2-1). The levels of total cholesterol and triglyceride in plasma were determined by enzymatic methods using the cholesterol assay kit and triglyceride assay kit, respectively (Stanbio Laboratory, Boerne, TX, USA). Plasma high-density lipoprotein cholesterol (HDL-C) and low-density lipoprotein cholesterol (LDL-C) concentrations were measured using Nanjing Jiancheng kits (Nanjing, Jiangsu, China, A112-1-1 and A113-1-1). The whole liver was isolated from individual mouse and weighed. 10% mice liver homogenate with normal saline solution was prepared in an ice-water bath. The superoxide dismutase (SOD) and catalase (CAT) activities of the liver samples were detected by SOD and CAT assay kits (Nanjing Jiancheng, Nanjing, Jiangsu, China, A001-3-2 and A007-1-1). Liver levels of malondialdehyde (MDA) were evaluated using the MDA assay kit (Nanjing Jiancheng, Nanjing, Jiangsu, China, A003-1-2). The liver glycogen contents were measured using a glycogen assay kit (Nanjing Jiancheng, Nanjing, Jiangsu, China, A043-1-1). A SpectraMax M5 microplate reader (Molecular Devices, Silicon Valley, CA, United States) was used to read the absorbance at the appropriate wavelength according to the instructions of the assay kits.

Histological examination

The fixed mouse liver paraffin sections (4 μm) were stained with hematoxylin and eosin (H&E) and Oil Red O. The areas of

Oil Red O staining in captured images were determined and quantified using Image-Pro Plus software (Media Cybernetics, Silver Spring, Md, USA). The glycogen content of the liver was examined by Periodic Acid–Schiff (PAS) staining. Histopathological changes were visualized under 200× magnification using microscopy.

Western blot assay

The treated HepG2 cells and liver samples isolated from mice after chronic treatments were lysed on ice with RIPA lysis buffer containing 1% Protease Inhibitor Cocktail and 1% phenylmethanesulfonyl fluoride (PMSF), both of which were obtained from Beyotime Biotechnology (Shanghai, China). Subsequently, lysates were centrifuged at 15 000 rpm for 30 min at 4 °C to collect supernatants. The BCA Protein assay kit (Beyotime, Shanghai, China) was used to measure the total protein contents. Equal concentrations (15 μg) of total proteins were separated using 8–10% SDS-PAGE gels (Bio-Rad, Hercules, CA, USA) and electrotransferred onto a polyvinylidene difluoride (PVDF) membrane (Millipore, Billerica, MA, USA). Nonfat milk powder (5%, Bio-Rad, Hercules, CA, USA) in Tris-buffered saline Tween (TBST) solution was utilized for blocking the membranes at room temperature. The membranes were incubated overnight with the appropriate primary antibodies at 4 °C. After washing 3 times with 1× TBST, the membranes were incubated with anti-rabbit or anti-mouse secondary antibodies for 2 h at room temperature. After washing 3 times with 1× TBST, protein bands were detected by enhanced chemiluminescence (ECL) detection solutions (Thermo Fisher, Waltham, MA, USA) using a ChemiDoc MP Imaging System (Bio-Rad, Hercules, CA, USA). Quantification of target protein levels was calculated using Image Lab (Bio-Rad, Hercules, CA, USA). The primary antibodies against GAPDH, IRS1, IRS2, p-IRS1 (Ser307), Akt, p-Akt (Ser 473), PI3K, GSK3β, p-GSK3β (Ser9), HO-1 and NQO1 were obtained from Cell Signalling Technology (Danvers, MA, USA); while Nrf2 was acquired from Beyotime Biotechnology (Shanghai, China). The secondary anti-rabbit antibodies and anti-mouse antibodies were obtained from Cell Signalling Technology (Danvers, MA, USA).

Statistical analysis

In this study, all the data were presented as mean ± S.E.M from three or more independent experiments. Differences between groups were analyzed using one-way analysis of variance (ANOVA) and Tukey's *post hoc* test with GraphPad Prism (GraphPad Software Inc., La Jolla, CA, USA). A p value < 0.05 was considered statistically significant difference.

Results

3,4′,5-TMS improves glucose consumption and glycogen synthesis in IR-HepG2 cells

The cytotoxicity of 3,4′,5-TMS on HepG2 at different concentrations (0.5–50 μM for 48 h) was evaluated by the MTT assay. The results showed that 3,4′,5-TMS had no observable toxic effects on HepG2 cells at low concentrations (0.5 and 1 μM) and 3,4′,5-TMS even slightly increased the cell viability of HepG2 cells at 0.5 μM. However, the cell viability significantly decreased at concentrations from 2.5 to 50 μM (Fig. 1A). Besides, the DMSO solvent at the same volume of 3,4′,5-TMS added did not affect the cell viability of HepG2 cells. Thus, the non-toxic concentrations of 3,4′,5-TMS at 0.5 and 1 μM were chosen for later experiments in this study.

To explore the potential effect of 3,4′,5-TMS on glucose consumption in IR-HepG2 cells, the glucose assay kit was used to measure the glucose concentration of cell culture supernatants. The concentration of glucose consumption of cells was obtained by subtracting the glucose concentration of medium with different treatments from the glucose concentration in the blank medium. As elucidated by the assay kit, HG and DXMS-treatment significantly decreased the glucose consumption of HepG2 cells as compared with the control group (Fig. 1B). 3,4′,5-TMS appeared to reverse the effect of high glucose and DXMS in HepG2 in a dose-dependent manner. In particular, 1 μM 3,4′,5-TMS significantly increased the glucose concentration of IR-HepG2 to a level comparable with control.

The results in Fig. 1C demonstrated that high glucose–DXMS treatment significantly reduced the intracellular glycogen content of IR-HepG2 cells as compared to control; and gly-

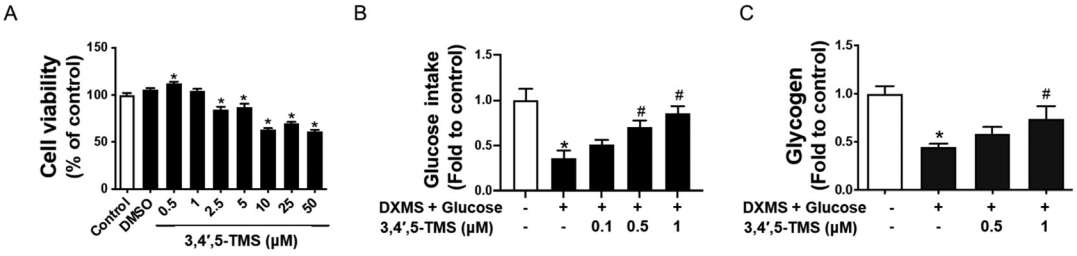

Fig. 1 3,4′,5-TMS improves glucose consumption and glycogen synthesis in high glucose-induced insulin resistant (IR)-HepG2 cells. (A) Cell viability in the HepG2 cells upon treatment with different concentrations of 3,4′,5-TMS for 48 h. (B) Glucose consumption and (C) glycogen content in IR-HepG2 cells pre-treated with high glucose (50 mM) plus dexamethasone (DXMS, 30 μM) for 48 h and treated with 3,4′,5-TMS for another 16 h. Values are the means ± SEM (n = 3); * p < 0.05 *vs*. control; # p < 0.05 *vs.* DXMS + glucose.

cogen synthesis was dose-dependently increased by 3,4′,5-TMS at 0.5 and 1 μM.

3,4′,5-TMS activates the IRS/PI3K/Akt insulin signaling pathway in IR-HepG2 cells

The western blotting assay was performed to study the action mechanism underlying the anti-diabetic activities of 3,4′,5-TMS. The IRS/PI3K/Akt pathway which plays a central role in insulin signaling was examined. In IR-HepG2 cells, the phosphorylation of IRS1 at Ser307 was up-regulated by the treatment of high glucose and DXMS; and such an increase was restored by 3,4′,5-TMS at 0.5 and 1 μM to a level comparable to control (Fig. 2A and B). At the same time, the protein levels of IRS1 and IRS2 were attenuated in IR-HepG2 cells. Conversely, 3,4′,5-TMS (1 μM) counteracted the effects of high glucose and DXMS to a level comparable with control (Fig. 2A, C and D). The PI3K/Akt signaling pathway was suppressed by the treatment of high glucose and DXMS: downregulated PI3K expression and reduced phosphorylation of Akt (p-Akt) at Ser473. These changes were remarkably prevented by 1 μM 3,4′,5-TMS while a lower concentration (0.5 μM) of 3,4′,5-TMS showed a moderate effect (Fig. 2A, E and F). To further explore the role of 3,4′,5-TMS in glycogen synthesis, western blot was performed to identify the protein level of total GSK3β and phosphorylation of GSK3β (p-GSK3β) at Ser9. Compared with the control group, high glucose–DXMS treatment significantly diminished p-GSK3β expression in HepG2 cells; and such reduction was reversed by 3,4′,5-TMS at 1 μM (Fig. 2A and G). The effect of 3,4′,5-TMS at 0.5 μM on the expression of p-GSK3β was not statistically significant.

3,4′,5-TMS alleviates oxidative stress by upregulating Nrf2 signaling

There is a tight linkage between IR and oxidative stress. The ROS generation of different groups was evaluated by CM-H2DCFDA to investigate the antioxidant capacity of 3,4′,5-TMS. In IR-HepG2 cells, the fluorescence intensity was stronger than in the control group, and the elevated ROS level was significantly reduced by 3,4′,5-TMS at both concentrations of 0.5 and 1 μM (Fig. 3A and B). Additionally, 3,4′,5-TMS increased the expression of Nrf2 and downstream proteins HO-1 and NQO1 in HG and DXMS-induced IR-HepG2 cells (Fig. 3C and D). All these results supported the antioxidant capacity of 3,4′,5-TMS.

Chronic 3,4′,5-TMS treatment improves blood glucose tolerance and the lipid profile in DIO mice

Based on the positive findings *in vitro*, we treated the DIO mice with 3,4′,5-TMS at 10 mg kg^{-1} day^{-1} for 4 weeks by oral gavage to investigate its effect *in vivo*. To examine the improvement of 3,4′,5-TMS treatment in metabolic disturbance, several important basic metabolic parameters were tested. The chronic 3,4′,5-TMS treatment to DIO mice had no effects on the body weight (Fig. 4A). The results of the oral glucose tolerance test (OGTT) and insulin tolerance test (ITT) presented in (Fig. 4B and C) showed that the sensitivities of glucose and insulin were diminished in DIO mice. These results together with the elevated fasting blood glucose indicated that at the 0 time point of OGTT (more than 11 mM) DIO mice developed diabetes. Oral administration of 3,4′,5-TMS did not alter the fasting blood glucose level but significantly improved glucose tolerance and insulin sensitivity in obese and diabetic mice. Compared with the control lean mice, chronic intake of a high-fat diet resulted in elevated plasma levels of total cholesterol (Fig. 4D), triglyceride (Fig. 4E) and LDL-C (Fig. 4F) whereas the level of HDL-C was not altered (Fig. 4G). 3,4′,5-TMS treatment effectively lowered the triglyceride level but the decreases in total cholesterol and LDL-C were insignificant. Besides, 3,4′,5-TMS administration increased the plasma level of HDL-C in DIO mice.

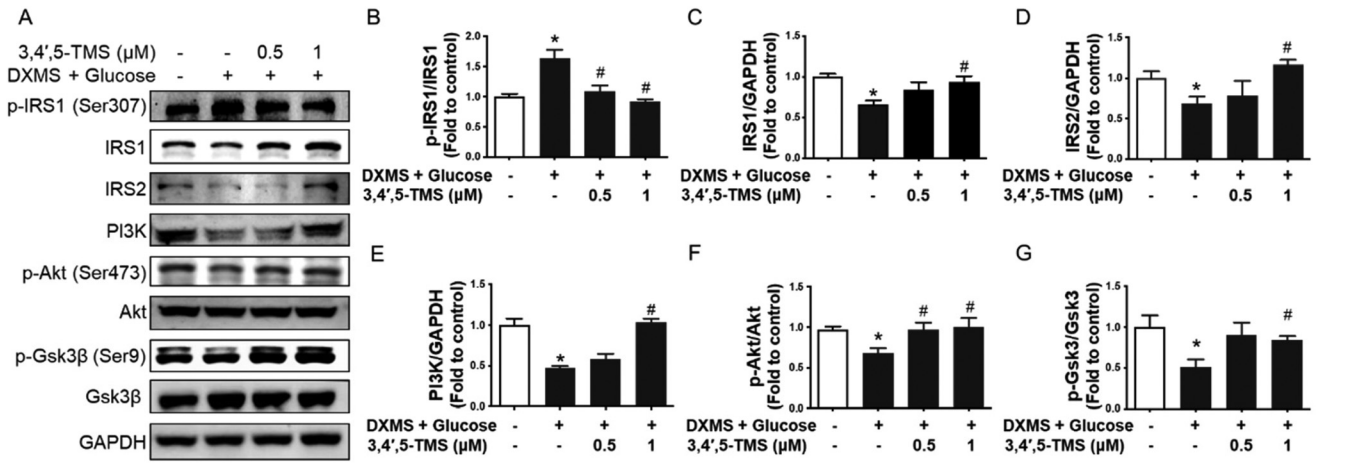

Fig. 2 3,4′,5-TMS activates the insulin signaling pathway in HepG2 cells. (A) Representative western blots and summarized data for protein levels of (B) phosphorylated IRS1 at Ser307 (180 kDa), (C) IRS1 (180 kDa), (D) IRS2 (185 kDa), (E) PI3K (85 kDa), (F) phosphorylated Akt at Ser473 (60 kDa), and (G) phosphorylated Gsk3β (46 kDa) compared to the corresponding total protein or GAPDH (37 kDa) in HepG2 cells with different treatments. Values are the means ± SEM (n = 4); * $p < 0.05$ *vs.* control; # $p < 0.05$ *vs.* DXMS + glucose.

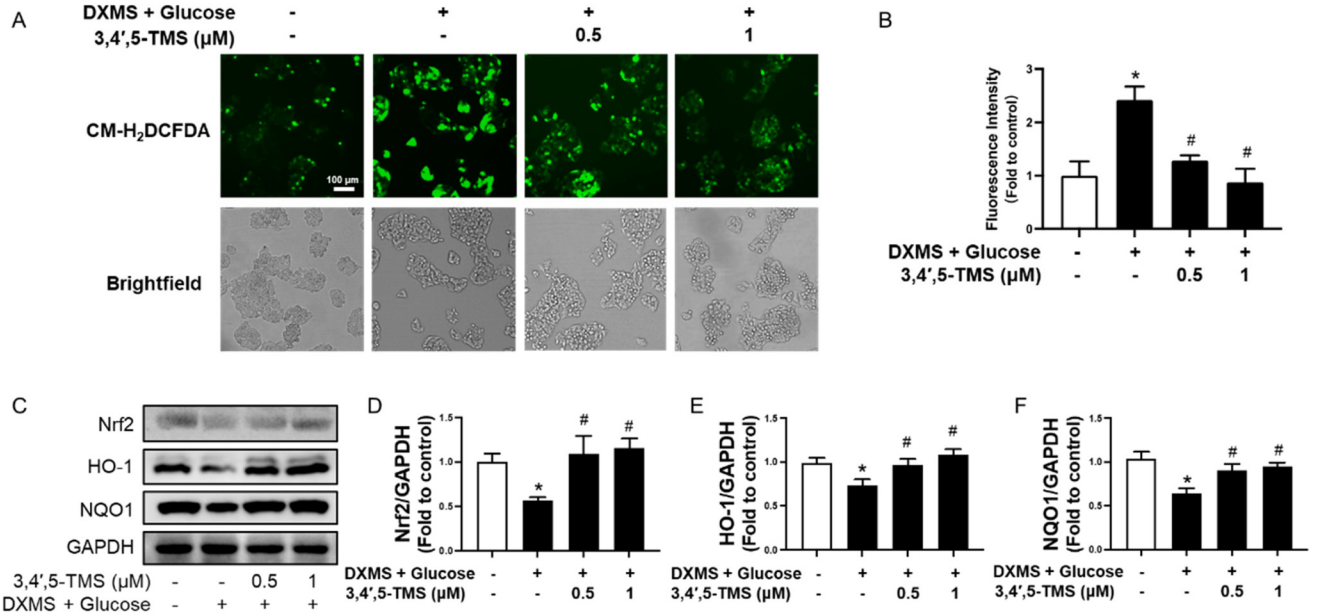

Fig. 3 3,4′,5-TMS suppresses oxidative stress in HepG2 cells. (A) Representative images and (B) summarized data showing the CM-H2DCFDA fluorescence intensity in IR-HepG2 cells pre-treated with high glucose (50 mM) plus DXMS (30 μM) for 48 h and treated with 3,4′,5-TMS for another 16 h. (C) Representative western blots and (D–F) summarized data for protein levels of Nrf2 (110 kDa), HO-1 (28 kDa) and NQO1 (29 kDa) in IR-HepG2 cells. Values are the means ± SEM (n = 4); * p < 0.05 *vs.* control; # p < 0.05 *vs.* DXMS + glucose.

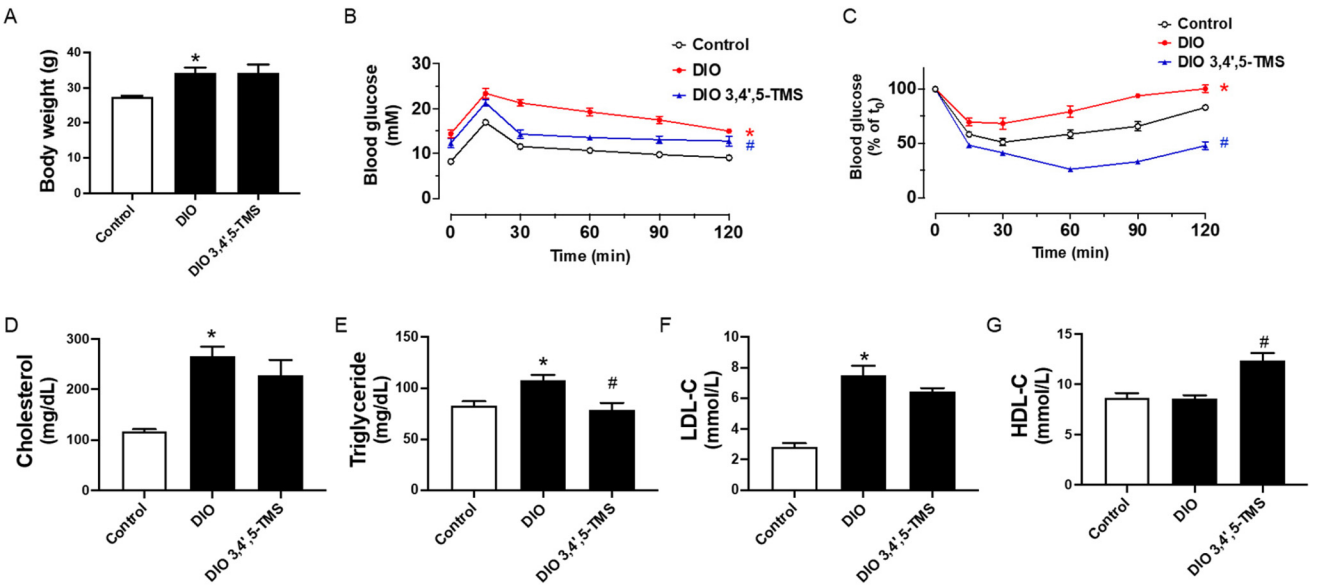

Fig. 4 Chronic 3,4′,5-TMS treatment enhances blood glucose and lipid modulations in high-fat diet-induced obese (DIO) mice. (A) Body weight, (B) oral glucose tolerance test (OGTT) upon 6 h of fasting, (C) insulin tolerance test (ITT) upon 2 h of fasting, and (D–G) plasma levels of total cholesterol, triglyceride, LDL-C and HDL-C in control lean mice and DIO mice administered with CMC–Na (vehicle) or 3,4′,5-TMS at 10 mg per kg body weight daily for 4 weeks. Values are the means ± SEM (n = 5–6); *p < 0.05, DIO *vs.* control; # p < 0.05, 3,4′,5-TMS *vs.* DIO.

3,4′,5-TMS treatment ameliorates fatty liver in DIO mice

3,4′,5-TMS did not affect the liver weight (Fig. 5A). The plasma ALT and AST contents and the histopathological manifestations of liver tissue were determined to evaluate the effect of 3,4′,5-TMS on liver damage in diabetes and obesity. The liver function of DIO mice was impaired, as evidenced by significantly increased ALT and AST in plasma (Fig. 5B and C). 3,4′,5-TMS ameliorated liver function as suggested by decreased levels of ALT and AST. Consistent with the above data, the liver segments from normal mice showed the regular structure of hepatocytes and the hepatic lobule. The cells are compactly

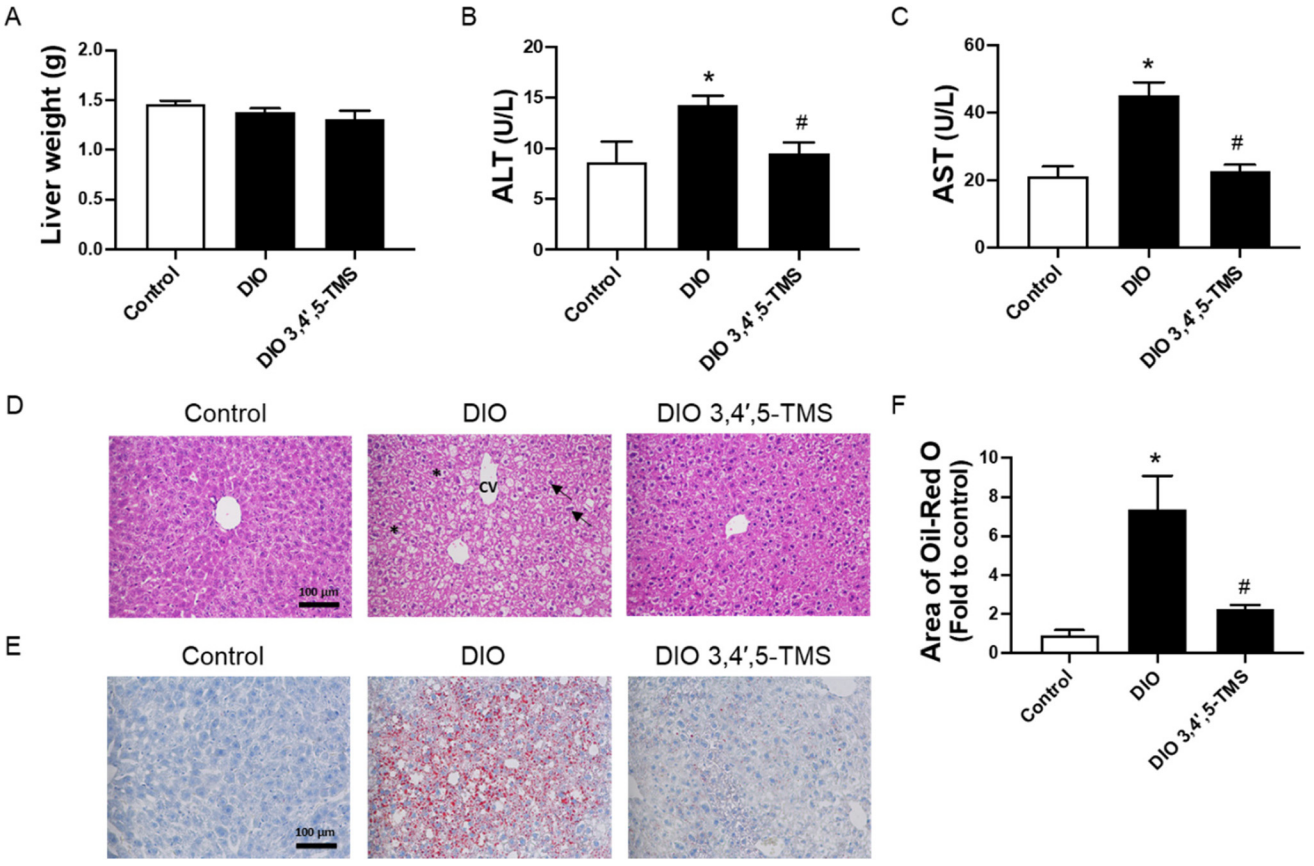

Fig. 5 Chronic 3,4′,5-TMS treatment alleviates fatty liver in DIO mice. (A) Liver weight, (B) alanine aminotransferase (ALT) and (C) aspartate aminotransferase (AST) in plasma, (D) H&E staining, (E) Oil Red O staining of the liver histological sections, and (F) calculated area of Oil Red O in different groups of mice treated with CMC–Na (vehicle) or 3,4′,5-TMS at 10 mg per kg body weight daily for 4 weeks. Values are the means ± SEM (n = 5–6); *p < 0.05, DIO *vs*. control; # p < 0.05, 3,4′,5-TMS *vs*. DIO. Central vein (cv); hepatocytes (arrow); vacuolization of the cytoplasm (*).

arranged and their structure is clear and intact (Fig. 5D). In contrast, the liver cells in the vehicle-treated obese mice were cloudy swelling and loosely arranged with vacuolization of the cytoplasm present. These histopathological changes in liver tissue were reversed by the treatment of 3,4′,5-TMS in DIO mice. Oil Red O staining showed that hepatic lipid accumulation was increased in obesity, which was suppressed by 3,4′,5-TMS treatment (Fig. 5E and F).

3,4′,5-TMS activates insulin signaling in the livers of DIO mice

To confirm the mechanism of action of 3,4′,5-TMS *in vivo*, protein levels of the IRS/PI3K/Akt pathway, including IRS1, IRS2, p-IRS1 at Ser307, PI3K, Akt, p-Akt at Ser473, p-GSK3β at Ser9 and GSK3β, were determined by western blot. In the livers of DIO mice, the protein levels of IRS1 and IRS2 were down-reregulated, accompanied by up-regulated phosphorylation of IRS1 at Ser307 (Fig. 6A–D). Such changes were significantly reversed by 3,4′,5-TMS treatment. The downstream expression of PI3K (Fig. 6E) and phosphorylation of Akt at Ser473 (Fig. 6F) were down-regulated. All these changes suppressed insulin signal transduction. Chronic 3,4′,5-TMS treatment reversed these changes, implying the activation of insulin signaling. 3,4′,5-TMS exerted a minor but insignificant effect in increasing PI3K expression.

As a substrate for Akt and a mediator of glycogen synthesis, GSK3β is inactivated upon phosphorylation at Ser9. Phosphorylation of GSK3β at Ser9 was down-regulated in DIO mice, which was increased by 3,4′,5-TMS treatment to a level comparable to lean control mice (Fig. 6G). PAS staining and a glycogen assay kit were used to further evaluate the effect of 3,4′,5-TMS on the hepatic glycogen synthesis ability in different treated mice. The area of PAS staining (magenta color) was decreased in DIO mice, showing that consumption of high-fat diet inhibited glycogen synthesis and storage capacity of the livers of mice (Fig. 6H). The glycogen assay kit also presented results consistent with PAS staining: glycogen concentrations in the livers of DIO mice were lower than those in control mice (Fig. 6I). Significantly, 3,4′,5-TMS treatment for 4 weeks mitigated these changes.

3,4′,5-TMS suppresses oxidative stress in the liver by upregulating Nrf2

A close association has been shown among oxidative stress, insulin resistance and liver injury, as described previously. The

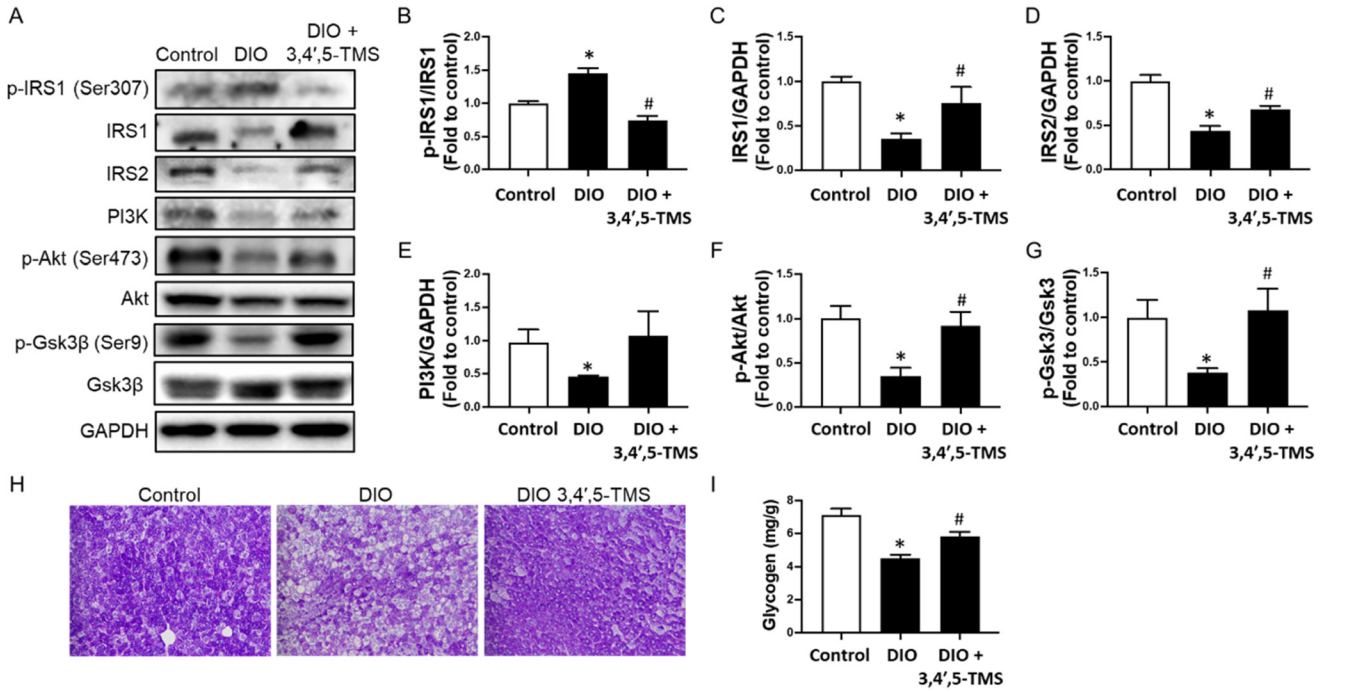

Fig. 6 Oral administration of 3,4′,5-TMS modulates the insulin signaling pathway and glycogen synthesis in livers *in vivo*. (A) Representative western blots and summarized data for protein levels of (B) phosphorylated IRS1 at Ser307 (180 kDa), (C) IRS1 (180 kDa), (D) IRS2 (185 kDa), (E) PI3K (85 kDa), (F) phosphorylated Akt at Ser473 (60 kDa), and (G) phosphorylated Gsk3β (46 kDa) compared to the corresponding total protein or GAPDH (37 kDa) in the livers from different groups of mice treated with CMC−Na (vehicle) or 3,4′,5-TMS at 10 mg per kg body weight daily for 4 weeks. (H) Representative images of periodic acid−Schiff (PAS) staining of the liver histological sections and (I) glycogen content in mouse livers. Values are the means ± SEM (n = 5−6); *p < 0.05, DIO *vs.* control; # p < 0.05, 3,4′,5-TMS *vs.* DIO.

CAT and SOD activities of the liver were decreased whilst the MDA level was increased in DIO mice (Fig. 7A–C). Chronic 3,4′,5-TMS treatment protected the liver from these effects induced by the long-term high-fat diet intake. Furthermore, the protein level of Nrf2 was significantly suppressed in the livers of DIO mice, which was restored by 3,4′,5-TMS to a comparable level with the control (Fig. 7D).

Discussion

The current study examined the anti-diabetes potential of 3,4′,5-TMS, and explored the mechanism modulating glucose homeostasis and oxidative stress in hepatic insulin resistance by using HG and DXMS-stimulated IR-HepG2 cells and DIO mice. The following findings were obtained *in vitro* and *in vivo*: (1) 3,4′,5-TMS treatment significantly improved the hepatic glucose metabolism through promoting glucose consumption and glycogen synthesis; (2) 3,4′,5-TMS treatment maintained glycemic sensing and insulin signaling by activating the IRS/PI3K/Akt pathway; and (3) 3,4′,5-TMS treatment protected the liver from oxidative stress induced by a high glucose and high-fat diet through Nrf2 activation of its downstream pathways.

Type 2 diabetes is a common chronic metabolic disease marked by insulin resistance and high blood glucose levels. Traditional treatments include oral medications, insulin injec-

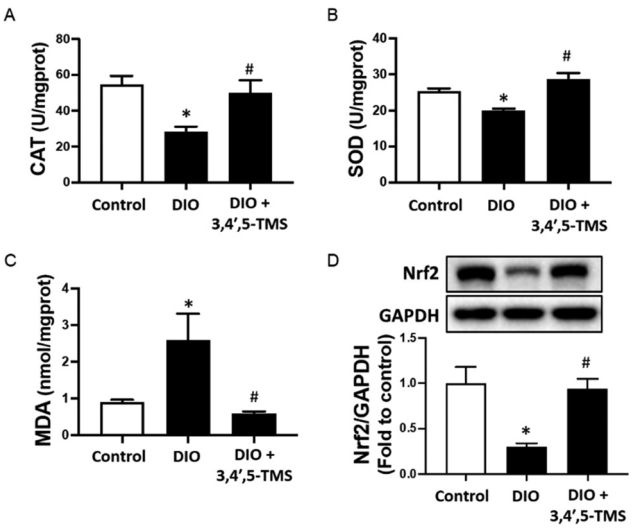

Fig. 7 Four-week 3,4′,5-TMS treatment on oxidative stress in the livers of DIO mice. Activities of (A) catalase (CAT) and (B) superoxide dismutase (SOD), and (C) malondialdehyde (MDA) and (D) Nrf2 protein levels (110 kDa) in the livers of different groups of mice with treatment of CMC−Na (vehicle) or 3,4′,5-TMS at 10 mg per kg body weight daily for 4 weeks. Values are the means ± SEM (n = 5−6); *p < 0.05, DIO *vs.* control; # p < 0.05, 3,4′,5-TMS *vs.* DIO.

tions, and lifestyle changes. However, these approaches face challenges in long-term blood sugar control and complication prevention, such as drug tolerance, side effects, and individual differences.[35] Safe and effective potential compounds for improving diabetes are being explored. Resveratrol has been extensively studied and well reported.[36,37] However, because of the hydrophobic scaffolds of polyphenols, oral administration of resveratrol has a very low bioavailability and a very short half-life in the circulatory system of humans.[38,39] In recent years, 3,4′,5-TMS, as a natural methoxy derivative of resveratrol, has become a strong candidate for anticancer with superior pharmacokinetic characteristics.[25] Therefore, the anti-diabetic effects of 3,4′,5-TMS were investigated for the first time in this study. The current study showed that 3,4′,5-TMS at concentrations from 2.5 to 50 μM significantly lowered the cell viability of HepG2 cells, which might be attributed to the anti-tumor potency of this resveratrol derivative. Low concentrations (0.5 and 1 μM) of 3,4′,5-TMS had no effect on cell viability. In the present study, oral administration of 3,4′,5-TMS at 10 mg per kg body weight daily for 4 weeks was safe for mice.

In T2DM, insulin resistance results in inhibition of the PI3K/Akt pathway which plays a central role in the mechanism of insulin transduction.[40] In healthy individuals, the pancreas secretes insulin in response to the elevated blood glucose after eating. Then, insulin binds with the insulin receptor and recruits IRS proteins to trigger the intracellular PI3K/Akt signaling cascade, regulating glucose uptake, glucose synthesis, gluconeogenesis, protein synthesis, cell growth and differentiation.[40,41] Notably, insulin resistance in the liver is related to the abundance and phosphorylation status of IRS1 and IRS2, which complement each other during metabolism.[42–44] Our results agreed well with previous studies wherein the expressions of IRS1 and IRS2 were decreased in the livers of diabetic mice, accompanied by the down-regulation of PI3K.[45] Another inhibition in insulin signaling involves the phosphorylation of IRS-1 at Ser307 by JNK activation.[46] Our *in vitro* and *in vivo* results supported that 3,4′,5-TMS regulated the IRS/PI3K/Akt pathway to potentially improve insulin resistance in diabetes.

In the liver, insulin activates glycogen synthesis and glycolysis and inhibits gluconeogenesis to reduce blood glucose concentration.[47,48] The regulation of glucose consumption and hepatic glycogen synthesis by IRS/PI3K/Akt signaling requires further regulation of downstream proteins.[49] GSK3β is inactivated by IRS/PI3K/Akt signaling-induced phosphorylation, and this inactivation subsequently reduces the inhibitory phosphorylation of glycogen synthase (GS), activating GS and thereby promoting glycogen synthesis.[50] Hepatic p-GSK3β expression was dramatically decreased in diabetes, consistent with the results reported by Chen *et al.*[51] In this study, we found that 3,4′,5-TMS was effective to normalize the blood glucose level by increasing the glucose consumption and glycogen synthesis with activated IRS/PI3K/Akt signaling and enhanced serine phosphorylation of GSK3β, improving insulin sensitivity and glucose tolerance *in vivo*. The results obtained from PAS staining and using the glycogen assay kit provided additional evidence supporting the therapeutic potential of 3,4′,5-TMS in the restoration of hepatic glycogen synthesis under conditions of insulin resistance.

Obesity and T2DM are closely related to each other. Chronic intake of a high-fat diet induces the development of diabetes, which is generally accompanied by obesity, increasing triglyceride and cholesterol productions.[52] T2DM patients commonly receive more risk of hyperlipidemia and fatty liver.[53] Meanwhile, insulin resistance causes blood glucose regulation disorders and lipid metabolism abnormalities. High levels of glucose and lipid accumulation will increase the burden on mitochondria to induce excessive generation of ROS, leading to oxidative stress and lipid peroxidation in the liver.[54,55] Oxidative stress causes liver damage through various mechanisms, including DNA damage, lipid peroxidation, protein oxidation, mitochondrial dysfunction, inflammatory response, and fibrosis.[56,57] These processes interact synergistically, creating a detrimental cycle that results in liver cell damage, heightened inflammatory response, and fibrosis progression. In the context of T2DM, the PI3K/Akt pathway is known to perform a key role in activating Nrf2 in response to oxidative stress.[58–60] It facilitates the dissociation of Nrf2 from Keap1, safeguarding Nrf2 from degradation. Simultaneously, it enhances the stability of Nrf2 and enables its translocation into the nucleus. In the nucleus, Nrf2 binds to the antioxidant response element (ARE) sequence, initiating the transcription of the downstream antioxidant and detoxification genes.[61] The Akt/GSK3β pathway influences Nrf2 activation.[62,63] Therefore, impaired PI3K/Akt/GSK3β signaling negatively affects the Nrf2-mediated antioxidant response, leading to increased oxidative stress in the liver. In this study, the expression of Nrf2 was significantly down-regulated in liver tissues from T2DM mice and high glucose-induced IR-HepG2 cells, in line with previous studies.[64,65] Resveratrol is demonstrated as an Nrf2 activator to increase the expression level of Nrf2 and has a potent antioxidant activity.[66,67] Consistently, our study showed that 3,4′,5-TMS protected the liver from oxidative stress damage by improving blood lipids and fatty liver, and reducing ROS levels *via* increasing Nrf2 expression which in turn induces the expression of downstream antioxidant factors, including HO-1, NQO1, CAT, and SOD. These enzymes collectively contribute to cellular antioxidant defense and provide protection against oxidative stress. At the same time, 3,4′,5-TMS diminished pathological changes of liver tissues, reducing fat accumulation in the livers of DIO mice. 3,4′,5-TMS effectively controlled oxidative stress and provided adequate antioxidant defense to protect the liver in T2DM.

Conclusions

The present study provides novel findings regarding the remarkable protective effect of 3,4′,5-TMS in response to T2DM. The results demonstrate that 3,4′,5-TMS exerts its beneficial effects by counteracting hepatic insulin resistance and oxidative stress, as shown through studies conducted in DXMS

and high glucose-induced IR-HepG2 cells *in vitro* and in a high-fat diet-induced obese diabetic mouse model *in vivo*. Notably, the compound activates key signaling pathways, including the IRS/PI3K/Akt and Nrf2/NQO1/HO-1 pathways, thus supporting its great potential as a therapeutic intervention for metabolic disorders in T2DM in various ways. Addressing the limitations of resveratrol, these findings highlight the broad prospects of 3,4′,5-TMS in improving T2DM, filling the research gap on 3,4′,5-TMS in T2DM. This finding is beneficial for expanding the scope for improving diabetes and providing new strategies for drug development.

Author contributions

Yi Tan: investigation, formal analysis, and writing – original draft. Chunxiu Zhou: investigation and formal analysis. Lingchao Miao: investigation. Xutao Zhang: investigation. Haroon Khan: writing – reviewing and editing. Baojun Xu: conceptualization and writing – reviewing and editing. Wai San Cheang: conceptualization, supervision, writing – reviewing and editing, and funding acquisition.

Conflicts of interest

There are no conflicts to declare.

Acknowledgements

This work was supported by the Science and Technology Development Fund, Macau SAR (005/2023/SKL) and the National Natural Science Foundation of China Young Scientists Fund (32200975; EF049/ICMS-CWS/2022/NSFC).

References

1 I. Kyrou, C. Tsigos, C. Mavrogianni, G. Cardon, V. Van Stappen, J. Latomme, J. Kivelä, K. Wikström, K. Tsochev, A. Nanasi, C. Semanova, R. Mateo-Gallego, I. Lamiquiz-Moneo, G. Dafoulas, P. Timpel, P. E. H. Schwarz, V. Iotova, T. Tankova, K. Makrilakis, Y. Manios, Y. Manios, G. Cardon, J. Lindström, P. Schwarz, K. Makrilakis, L. Annemans, I. Garamendi, M. Kontogianni, O. Androutsos, C. Mavrogianni, K. Tsoutsoulopoulou, C. Katsarou, E. Karaglani, I. Qira, E. Skoufas, K. Maragkopoulou, A. Tsiafitsa, I. Sotiropoulou, M. Tsolakos, E. Argyri, M. Nikolaou, E.-A. Vampouli, C. Filippou, K. Gatsiou, E. Dimitriadis, T. Laatikainen, K. Wikström, J. Kivelä, P. Valve, E. Levälahti, E. Virtanen, R. Willems, I. Panchyrz, M. Holland, P. Timpel, S. Liatis, G. Dafoulas, C.-P. Lambrinou, A. Giannopoulou, L. Tsirigoti, E. Fappa, C. Anastasiou, K. Zachari, L. Rabemananjara, M. S. de Sabata, W. Ko, L. Moreno, F. Civeira, G. Bueno, P. De Miguel-Etayo, E. M. Gonzalez-Gil, M. I. Mesana, G. Vicente-Rodriguez, G. Rodriguez, L. Baila-Rueda, A. Cenarro, E. Jarauta, R. Mateo-Gallego, V. Iotova, T. Tankova, N. Usheva, K. Tsochev, N. Chakarova, S. Galcheva, R. Dimova, Y. Bocheva, Z. Radkova, V. Marinova, Y. Bazdarska, T. Stefanova, I. Rurik, T. Ungvari, Z. Jancsó, A. Nánási, L. Kolozsvári, C. Semánova, R. Martinez, M. Tong, K. Joutsenniemi, K. Wendel-Mitoraj and G. on behalf of the Feel4Diabetes-study, Sociodemographic and lifestyle-related risk factors for identifying vulnerable groups for type 2 diabetes: a narrative review with emphasis on data from Europe, *BMC Endocr. Disord.*, 2020, **20**, 134.

2 Y. Zheng, S. H. Ley and F. B. Hu, Global aetiology and epidemiology of type 2 diabetes mellitus and its complications, *Nat. Rev. Endocrinol.*, 2018, **14**, 88–98.

3 M. C. Riddle and W. H. Herman, The cost of diabetes care—an elephant in the room, *Diabetes Care*, 2018, **41**, 929–932.

4 M. P. Czech, Insulin action and resistance in obesity and type 2 diabetes, *Nat. Med.*, 2017, **23**, 804–814.

5 B. Ahmed, R. Sultana and M. W. Greene, Adipose tissue and insulin resistance in obese, *Biomed. Pharmacother.*, 2021, **137**, 111315.

6 R. Meshkani and K. Adeli, Hepatic insulin resistance, metabolic syndrome and cardiovascular disease, *Clin. Biochem.*, 2009, **42**, 1331–1346.

7 D. Akshintala, R. Chugh, F. Amer and K. Cusi, *Nonalcoholic fatty liver disease: the overlooked complication of type 2 diabetes*, 2019.

8 C. Faselis, A. Katsimardou, K. Imprialos, P. Deligkaris, M. Kallistratos and K. Dimitriadis, Microvascular complications of type 2 diabetes mellitus, *Curr. Vasc. Pharmacol.*, 2020, **18**, 117–124.

9 S. Schinner, W. Scherbaum, S. Bornstein and A. Barthel, Molecular mechanisms of insulin resistance, *Diabetic Med.*, 2005, **22**, 674–682.

10 E. Świderska, J. Strycharz, A. Wróblewski, J. Szemraj, J. Drzewoski and A. Śliwińska, Role of PI3K/AKT pathway in insulin-mediated glucose uptake, *Blood Glucose Levels*, 2018, **1**, 1–18.

11 S. S. Eckstein, C. Weigert and R. Lehmann, Divergent Roles of IRS (Insulin Receptor Substrate) 1 and 2 in Liver and Skeletal Muscle, *Curr. Med. Chem.*, 2017, **24**, 1827–1852.

12 C. M. Taniguchi, B. Emanuelli and C. R. Kahn, Critical nodes in signalling pathways: insights into insulin action, *Nat. Rev. Mol. Cell Biol.*, 2006, **7**, 85–96.

13 V. Aguirre, E. D. Werner, J. Giraud, Y. H. Lee, S. E. Shoelson and M. F. White, Phosphorylation of Ser307 in Insulin Receptor Substrate-1 Blocks Interactions with the Insulin Receptor and Inhibits Insulin Action*, *J. Biol. Chem.*, 2002, **277**, 1531–1537.

14 H. Li, Y. Yang, Z. Mo, Y. Ding and W. Jiang, Silibinin improves palmitate-induced insulin resistance in C2C12 myotubes by attenuating IRS-1/PI3K/Akt pathway inhibition, *Braz. J. Med. Biol. Res.*, 2015, **48**, 440–446.

15 Y. Tan, M. S. Cheong and W. S. Cheang, Roles of Reactive Oxygen Species in Vascular Complications of Diabetes:

Therapeutic Properties of Medicinal Plants and Food, *Oxygen*, 2022, **2**, 246–268.

16 L. V. Yuzefovych, S. I. Musiyenko, G. L. Wilson and L. I. Rachek, Mitochondrial DNA damage and dysfunction, and oxidative stress are associated with endoplasmic reticulum stress, protein degradation and apoptosis in high fat diet-induced insulin resistance mice, *PLoS One*, 2013, **8**, e54059.

17 S. Tangvarasittichai, Oxidative stress, insulin resistance, dyslipidemia and type 2 diabetes mellitus, *World J. Diabetes*, 2015, **6**, 456–480.

18 Y. Wang, X. Miao, J. Sun and L. Cai, Oxidative Stress in Diabetes: Molecular basis for diet supplementation, *Molecular Nutrition and Diabetes*, 2015, 65–72.

19 M. Thiruvengadam, B. Venkidasamy, U. Subramanian, R. Samynathan, M. Ali Shariati, M. Rebezov, S. Girish, S. Thangavel, A. R. Dhanapal, N. Fedoseeva, J. Lee and I.-M. Chung, Bioactive Compounds in Oxidative Stress-Mediated Diseases: Targeting the NRF2/ARE Signaling Pathway and Epigenetic Regulation, *Antioxidants*, 2021, **10**, 1859.

20 S. Li, N. Eguchi, H. Lau and H. Ichii, The Role of the Nrf2 Signaling in Obesity and Insulin Resistance, *Int. J. Mol. Sci.*, 2020, **21**, 6973.

21 T. A. Beyer, W. Xu, D. Teupser, U. auf dem Keller, P. Bugnon, E. Hildt, J. Thiery, Y. W. Kan and S. Werner, Impaired liver regeneration in Nrf2 knockout mice: role of ROS–mediated insulin/IGF–1 resistance, *EMBO J.*, 2008, **27**, 212–223.

22 J. A. David, W. J. Rifkin, P. S. Rabbani and D. J. Ceradini, The Nrf2/Keap1/ARE Pathway and Oxidative Stress as a Therapeutic Target in Type II Diabetes Mellitus, *J. Diabetes Res.*, 2017, **2017**, 4826724.

23 W. S. Cheang, W. T. Wong, L. Wang, C. K. Cheng, C. W. Lau, R. C. W. Ma, A. M. Xu, N. P. Wang, Y. Huang and X. Y. Tian, Resveratrol ameliorates endothelial dysfunction in diabetic and obese mice through sirtuin 1 and peroxisome proliferator-activated receptor delta, *Pharmacol. Res.*, 2019, **139**, 384–394.

24 C. K. Cheng, J. Y. Luo, C. W. Lau, Z. Y. Chen, X. Y. Tian and Y. Huang, Pharmacological basis and new insights of resveratrol action in the cardiovascular system, *Br. J. Pharmacol.*, 2020, **177**, 1258–1277.

25 F. S. Aldawsari and C. A. Velázquez-Martínez, 3,4′,5-trans-Trimethoxystilbene; a natural analogue of resveratrol with enhanced anticancer potency, *Invest. New Drugs*, 2015, **33**, 775–786.

26 X. Wen and T. Walle, Methylated flavonoids have greatly improved intestinal absorption and metabolic stability, *Drug Metab. Dispos.*, 2006, **34**, 1786–1792.

27 W. Nawaz, Z. Zhou, S. Deng, X. Ma, X. Ma, C. Li and X. Shu, Therapeutic versatility of resveratrol derivatives, *Nutrients*, 2017, **9**, 1188.

28 C. Zhou, Y. Tan, B. Xu, Y. Wang and W.-S. Cheang, 3, 4′, 5-Trimethoxy-trans-stilbene Alleviates Endothelial Dysfunction in Diabetic and Obese Mice via Activation of the AMPK/SIRT1/eNOS Pathway, *Antioxidants*, 2022, **11**, 1286.

29 C. Zhou, X. Zhang, C.-C. Ruan and W. S. Cheang, Two methoxy derivatives of resveratrol, 3,3′,4,5′-tetramethoxy-trans-stilbene and 3,4′,5-trimethoxy-trans-stilbene, suppress lipopolysaccharide-induced inflammation through inactivation of MAPK and NF-κB pathways in RAW 264.7 cells, *Chin. Med.*, 2021, **16**, 69.

30 B. Liu, X.-J. Luo, Z.-B. Yang, J.-J. Zhang, T.-B. Li, X.-J. Zhang, Q.-L. Ma, G.-G. Zhang, C.-P. Hu and J. Peng, Inhibition of NOX/VPO1 pathway and inflammatory reaction by trimethoxystilbene in prevention of cardiovascular remodeling in hypoxia-induced pulmonary hypertensive rats, *J. Cardiovasc. Pharmacol.*, 2014, **63**, 567–576.

31 Y. Feng, J. Clayton, W. Yake, J. Li, W. Wang, L. Winne and M. Hong, Resveratrol Derivative, Trans-3, 5, 4′-Trimethoxystilbene Sensitizes Osteosarcoma Cells to Apoptosis via ROS-Induced Caspases Activation, *Oxid. Med. Cell. Longevity*, 2021, **2021**, 8840692.

32 Y. Tan, L. Miao, J. Xiao and W. S. Cheang, 3,3′,4,5′-Tetramethoxy-trans-stilbene Improves Insulin Resistance by Activating the IRS/PI3K/Akt Pathway and Inhibiting Oxidative Stress, *Curr. Issues Mol. Biol.*, 2022, **44**, 2175–2185.

33 L. C. Miao, H. L. Zhang, M. S. Cheong, R. T. Zhong, P. Garcia-Oliveira, M. A. Prieto, K. W. Cheng, M. F. Wang, H. Cao, S. P. Nie, J. Simal-Gandara, W. San Cheang and J. B. Xiao, Anti-diabetic potential of apigenin, luteolin, and baicalein via partially activating PI3K/Akt/GLUT-4 signaling pathways in insulin-resistant HepG2 cells, *Food Sci. Hum. Wellness*, 2023, **12**, 1991–2000.

34 C. Beaupere, A. Liboz, B. Fève, B. Blondeau and G. Guillemain, Molecular mechanisms of glucocorticoid-induced insulin resistance, *Int. J. Mol. Sci.*, 2021, **22**, 623.

35 Y. Wu, Y. Ding, Y. Tanaka and W. Zhang, Risk factors contributing to type 2 diabetes and recent advances in the treatment and prevention, *Int. J. Med. Sci.*, 2014, **11**, 1185.

36 M. J. Nanjan and J. Betz, Resveratrol for the Management of Diabetes and its Downstream Pathologies, *Eur. Endocrinol.*, 2014, **10**, 31–35.

37 D. Sinha, N. Sarkar, J. Biswas and A. Bishayee, Resveratrol for breast cancer prevention and therapy: Preclinical evidence and molecular mechanisms, *Semin. Cancer Biol.*, 2016, **40–41**, 209–232.

38 D. Perrone, M. P. Fuggetta, F. Ardito, A. Cottarelli, A. De Filippis, G. Ravagnan, S. De Maria and L. Lo Muzio, Resveratrol (3,5,4′-trihydroxystilbene) and its properties in oral diseases, *Exp. Ther. Med.*, 2017, **14**, 3–9.

39 T. Walle, F. Hsieh, M. H. DeLegge, J. E. Oatis Jr. and U. K. Walle, High absorption but very low bioavailability of oral resveratrol in humans, *Drug Metab. Dispos.*, 2004, **32**, 1377–1382.

40 X. Huang, G. Liu, J. Guo and Z. Su, The PI3K/AKT pathway in obesity and type 2 diabetes, *Int. J. Biol. Sci.*, 2018, **14**, 1483.

41 M. S. Rahman, K. S. Hossain, S. Das, S. Kundu, E. O. Adegoke, M. A. Rahman, M. A. Hannan, M. J. Uddin

and M.-G. Pang, Role of insulin in health and disease: an update, *Int. J. Mol. Sci.*, 2021, **22**, 6403.

42 K. D. Copps and M. F. White, Regulation of insulin sensitivity by serine/threonine phosphorylation of insulin receptor substrate proteins IRS1 and IRS2, *Diabetologia*, 2012, **55**, 2565–2582.

43 E. B. Arias, L. E. Gosselin and G. D. Cartee, Exercise Training Eliminates Age-Related Differences in Skeletal Muscle Insulin Receptor and IRS-1 Abundance in Rats, *J. Gerontol., Ser. A*, 2001, **56**, B449–B455.

44 Y. Kido, D. J. Burks, D. Withers, J. C. Bruning, C. R. Kahn, M. F. White and D. Accili, Tissue-specific insulin resistance in mice with mutations in the insulin receptor, IRS-1, and IRS-2, *J. Clin. Invest.*, 2000, **105**, 199–205.

45 N. J. Kerouz, D. Hörsch, S. Pons and C. R. Kahn, Differential regulation of insulin receptor substrates-1 and-2 (IRS-1 and IRS-2) and phosphatidylinositol 3-kinase isoforms in liver and muscle of the obese diabetic (ob/ob) mouse, *J. Clin. Invest.*, 1997, **100**, 3164–3172.

46 W. Sun, Y. Bi, H. Liang, M. Cai, X. Chen, Y. Zhu, M. Li, F. Xu, Q. Yu, X. He, J. Ye and J. Weng, Inhibition of obesity-induced hepatic ER stress by early insulin therapy in obese diabetic rats, *Endocrine*, 2011, **39**, 235–241.

47 M. M. Qaid and M. M. Abdelrahman, Role of insulin and other related hormones in energy metabolism—A review, *Cogent Food Agric.*, 2016, **2**, 1267691.

48 M. Hatting, C. D. J. Tavares, K. Sharabi, A. K. Rines and P. Puigserver, Insulin regulation of gluconeogenesis, *Ann. N. Y. Acad. Sci.*, 2018, **1411**, 21–35.

49 A. Chadt and H. Al-Hasani, Glucose transporters in adipose tissue, liver, and skeletal muscle in metabolic health and disease, *Pfluegers Arch.*, 2020, **472**, 1273–1298.

50 E. J. McManus, K. Sakamoto, L. J. Armit, L. Ronaldson, N. Shpiro, R. Marquez and D. R. Alessi, Role that phosphorylation of GSK3 plays in insulin and Wnt signalling defined by knockin analysis, *EMBO J.*, 2005, **24**, 1571–1583.

51 L. Chen, X. Lin, X. Fan, Y. Qian, Q. Lv and H. Teng, Sonchus oleraceus Linn extract enhanced glucose homeostasis through the AMPK/Akt/GSK-3β signaling pathway in diabetic liver and HepG2 cell culture, *Food Chem. Toxicol.*, 2020, **136**, 111072.

52 M. Lai, P. C. Chandrasekera and N. D. Barnard, You are what you eat, or are you? The challenges of translating high-fat-fed rodents to human obesity and diabetes, *Nutr. Diabetes*, 2014, **4**, e135–e135.

53 F. G. S. Toledo, A. D. Sniderman and D. E. Kelley, Influence of Hepatic Steatosis (Fatty Liver) on Severity and Composition of Dyslipidemia in Type 2 Diabetes, *Diabetes Care*, 2006, **29**, 1845–1850.

54 J. Mohamed, A. H. Nazratun Nafizah, A. H. Zariyantey and S. B. Budin, Mechanisms of Diabetes-Induced Liver Damage: The role of oxidative stress and inflammation, *Sultan Qaboos Univ. Med. J.*, 2016, **16**, e132–e141.

55 C. Feillet-Coudray, E. Rock, C. Coudray, K. Grzelkowska, V. Azais-Braesco, D. Dardevet and A. Mazur, Lipid peroxidation and antioxidant status in experimental diabetes, *Clin. Chim. Acta*, 1999, **284**, 31–43.

56 A. Allameh, R. Niayesh-Mehr, A. Aliarab, G. Sebastiani and K. Pantopoulos, Oxidative stress in liver pathophysiology and disease, *Antioxidants*, 2023, **12**, 1653.

57 S. Li, H.-Y. Tan, N. Wang, Z.-J. Zhang, L. Lao, C.-W. Wong and Y. Feng, The role of oxidative stress and antioxidants in liver diseases, *Int. J. Mol. Sci.*, 2015, **16**, 26087–26124.

58 V. R. Pasupuleti, C. S. Arigela, S. H. Gan, S. K. N. Salam, K. T. Krishnan, N. A. Rahman and M. S. Jeffree, A Review on Oxidative Stress, Diabetic Complications, and the Roles of Honey Polyphenols, *Oxid. Med. Cell. Longevity*, 2020, **2020**, 8878172.

59 R. Subba, M. H. Ahmad, B. Ghosh and A. C. Mondal, Targeting NRF2 in Type 2 diabetes mellitus and depression: Efficacy of natural and synthetic compounds, *Eur. J. Pharmacol.*, 2022, **925**, 174993.

60 J. Duan, Y. Zhao, F. Pei, W. Deng, L. He, C. Rao, Y. Zhai and C. Zhang, Swietenine inhibited oxidative stress through AKT/Nrf2/HO–1 signal pathways and the liver–protective effect in T2DM mice: In vivo and in vitro study, *Environ. Toxicol.*, 2023, **38**, 1292–1304.

61 Y. Li, Y. Guo, Z. Feng, R. Bergan, B. Li, Y. Qin, L. Zhao, Z. Zhang and M. Shi, Involvement of the PI3K/Akt/Nrf2 Signaling Pathway in Resveratrol-Mediated Reversal of Drug Resistance in HL-60/ADR Cells, *Nutr. Cancer*, 2019, 1–12.

62 Y. Lv, H. Jiang, S. Li, B. Han, Y. Liu, D. Yang, J. Li, Q. Yang, P. Wu and Z. Zhang, Sulforaphane prevents chromium-induced lung injury in rats via activation of the Akt/GSK-3beta/Fyn pathway, *Environ. Pollut.*, 2020, **259**, 113812.

63 B. Liu, H. Jiang, J. Lu, R. Baiyun, S. Li, Y. Lv, D. Li, H. Wu and Z. Zhang, Grape seed procyanidin extract ameliorates lead-induced liver injury via miRNA153 and AKT/GSK-3beta/Fyn-mediated Nrf2 activation, *J. Nutr. Biochem.*, 2018, **52**, 115–123.

64 J. Chen, Z. Zhang and L. Cai, Diabetic cardiomyopathy and its prevention by nrf2: current status, *Diabetes Metab. J.*, 2014, **38**, 337–345.

65 X. Ding, T. Jian, Y. Wu, Y. Zuo, J. Li, H. Lv, L. Ma, B. Ren, L. Zhao, W. Li and J. Chen, Ellagic acid ameliorates oxidative stress and insulin resistance in high glucose-treated HepG2 cells via miR-223/keap1-Nrf2 pathway, *Biomed. Pharmacother.*, 2019, **110**, 85–94.

66 E. N. Kim, J. H. Lim, M. Y. Kim, T. H. Ban and B. S. Choi, Resveratrol, an Nrf2 activator, ameliorates aging-related progressive renal injury, *Aging*, 2018, **10**, 83–99.

67 S. H. Shahcheraghi, F. Salemi, S. Small, S. Syed, F. Salari, W. Alam, W. S. Cheang, L. Saso and H. Khan, Resveratrol regulates inflammation and improves oxidative stress via Nrf2 signaling pathway: Therapeutic and biotechnological prospects, *Phytother. Res.*, 2023, **37**, 1590–1605.